



HAL
open science

Truncated QR factorization with pivoting in mixed precision

Alfredo Buttari, Théo Mary, André Pachteau

► **To cite this version:**

Alfredo Buttari, Théo Mary, André Pachteau. Truncated QR factorization with pivoting in mixed precision. 2024. hal-04490215

HAL Id: hal-04490215

<https://hal.science/hal-04490215>

Preprint submitted on 5 Mar 2024

HAL is a multi-disciplinary open access archive for the deposit and dissemination of scientific research documents, whether they are published or not. The documents may come from teaching and research institutions in France or abroad, or from public or private research centers.

L'archive ouverte pluridisciplinaire **HAL**, est destinée au dépôt et à la diffusion de documents scientifiques de niveau recherche, publiés ou non, émanant des établissements d'enseignement et de recherche français ou étrangers, des laboratoires publics ou privés.



Distributed under a Creative Commons Attribution - NonCommercial 4.0 International License



Institut de Recherche en Informatique de Toulouse
CNRS - INP - UT3 - UT1 - UT2J

Truncated QR factorization with pivoting in mixed precision

Alfredo Buttari*

IRIT, Toulouse University, CNRS, INP, UT3, Toulouse, France
alfredo.buttari@irit.fr

Theo Mary*

Sorbonne Université, CNRS, LIP6, Paris, France
theo.mary@lip6.fr

André Pachteau*

IRIT, Toulouse University, CNRS, INP, UT3, Toulouse, France
andre.pachteau@gmail.com

* contact authors

01 March 2024

Working document
(version 1)



Institut de Recherche en Informatique de Toulouse
CNRS - INP - UT3 - UT1 - UT2J

Truncated QR factorization with pivoting in mixed precision

Alfredo Buttari*

IRIT, Toulouse University, CNRS, INP, UT3, Toulouse, France
alfredo.buttari@irit.fr

Theo Mary*

Sorbonne Université, CNRS, LIP6, Paris, France
theo.mary@lip6.fr

André Pachteau*

IRIT, Toulouse University, CNRS, INP, UT3, Toulouse, France
andre.pachteau@gmail.com

* contact authors

01 March 2024

Abstract. Low-rank approximations are widely used to reduce the memory footprint and operational complexity of numerous linear algebra algorithms in scientific computing and data analysis. In some of our recent work we have demonstrated that low-rank approximations can be stored using multiple arithmetic precisions to further reduce the storage and execution time. In this work we present a method that can produce this mixed-precision representation directly; this relies on a mixed-precision truncated rank-revealing QR (RRQR) factorization with pivoting. We present a floating-point error analysis and provide bounds on the error of the approximation demonstrating that the use of multiple precisions does not alter the overall accuracy. Finally, we present experimental results showing the execution time reduction for the cases where either classical or randomized pivoting are used.

Keywords: Mixed-precision, QR factorization, low-rank approximations

Working document
(version 1)



Institut de Recherche en Informatique de Toulouse
CNRS - INP - UT3 - UT1 - UT2J

Factorisation QR avec pivotage et troncature en précision mixte

Alfredo Buttari*

IRIT, Université de Toulouse, CNRS, INP, UT3, Toulouse, France
alfredo.buttari@irit.fr

Theo Mary*

Sorbonne Université, CNRS, LIP6, Paris, France
theo.mary@lip6.fr

André Pacteau*

IRIT, Université de Toulouse, CNRS, INP, UT3, Toulouse, France
andre.pacteau@gmail.com

* contact authors

01 Mars 2024

Résumé. Les approximations de rang faible sont couramment utilisées pour réduire la consommation de mémoire et la complexité calculatoire de nombreux algorithmes d'algèbre linéaire en calcul scientifique et analyse des données. Dans nos travaux récents, nous avons démontré que les approximations de rang faible peuvent être stockées en utilisant de multiples précisions arithmétiques pour réduire d'avantage la mémoire et le temps d'exécution. Dans ce document, nous présentons une nouvelle méthode qui produit directement ces représentations; elle repose sur une factorisation QR en précision mixte tronquée et avec pivotage. Nous présentons une analyse des erreurs d'arrondi en virgule flottante ainsi que des bornes pour l'erreur d'approximation montrant que l'utilisation de plusieurs précisions ne dégrade pas la qualité de la solution finale. Finalement, nous présentons des résultats expérimentaux montrant la réduction du temps d'exécution obtenue avec les méthodes proposées.

Mots-clés : Mixed-precision, QR factorization, low-rank approximations

Document de travail
(version 1)

Contents

1 Introduction	1
2 Background	2
2.1 Householder QR and error analysis.	3
2.2 QR factorization with Businger-Golub pivoting	5
2.3 QR factorization with randomized pivoting	6
3 Error analysis	6
4 Pivoted QR factorization in mixed precision	9
4.1 Truncated QR factorization with Businger-Golub pivoting	10
4.2 Truncated QR factorization with randomized pivoting	10
4.3 Truncated QR factorization in mixed precision	11
5 Numerical experiments	11
5.1 Theory validation with a Julia prototype	12
5.2 Performance analysis with optimized code	15
6 Conclusions and future work	17
7 Acknowledgments.	17

1 Introduction

Alongside many classical applications in data analysis, the use of low-rank approximations in computing has become increasingly popular in recent years due to their effectiveness in reducing both the memory consumption and the operational complexity of numerous linear algebra algorithms such as linear system solvers [2, 20, 11]. Essentially, these rely on the idea that a matrix $A \in \mathbb{R}^{m \times n}$ can be approximately represented as a product XY^T where $X \in \mathbb{R}^{m \times k}$ and $Y \in \mathbb{R}^{n \times k}$ are matrices of sufficiently low rank k such that

$$\|A - XY^T\| \leq \varepsilon \|A\|$$

in some norm, where ε is a prescribed accuracy tolerance. For a given ε an optimal approximation can be obtained by computing the singular value decomposition of A and dropping all the singular values smaller than ε and the corresponding left and right singular vectors [10]. Nevertheless, this method is rarely used in practice due to its high cost and low efficiency. Instead, other methods are preferred which are sufficiently accurate and robust in practice, and more computationally efficient and/or scalable in a parallel setting; among these, we can cite rank-revealing QR factorizations [4] or randomized approaches [18].

Concurrently, low-precision floating-point arithmetic units have become increasingly available and supported not only in specialized computing platforms (such as GPUs) but also in commodity CPUs. This is partly due to the recent explosion of artificial intelligence and machine learning algorithms in science and engineering which work remarkably well with low (e.g., 16-bit) or even very low (8-bit) precisions. As a result, new floating-point arithmetic formats have been proposed and, sometimes, standardized, such as binary16 or BFloat16 which can achieve higher performance than the traditional 32-bit or 64-bit floating-point formats. Despite their wide adoption in machine learning, these low-precision formats cannot be straightforwardly employed in applications which require relatively high accuracy; this has reignited the interest of the scientific computing

community around mixed-precision algorithms. These combine multiple arithmetic formats in order to achieve provably accurate results while maximizing the use of low-precision units in order to improve performance. In particular, in our recent work [1] we have demonstrated that low-rank approximations can be stored in a mixed-precision format which can then be used in a direct method to solve linear systems of equations in a backward stable way. This approach amounts to partitioning the columns of X and Y into block-columns such that the overall accuracy of the approximation

$$\|A - X^1 Y^{1T} - \dots - X^p Y^{pT}\| \leq \varepsilon \|A\| \quad (1)$$

is still satisfied when the X^i and Y^i data are stored, from left to right, using different arithmetics of decreasing precision. Intuitively, this can be explained by the fact that the rightmost columns of X and Y are associated with small singular values which carry little information and play a minor role in the error of the low-rank approximation. This splitting is dictated by the spectrum of A , the number and accuracy of the p available precisions and the threshold ε . In the same work we have demonstrated that this mixed-precision format can be used to reduce the execution time of matrix factorizations without harming the backward stability. The format in equation (1) can straightforwardly be obtained by first computing the low-rank approximation fully in high precision and then by appropriately casting the block-columns of X and Y into lower precisions; nevertheless, using this naive approach leads to poor performance in contexts where computing the high precision low-rank approximation is the bottleneck.

In the present work, we propose a mixed-precision pivoted QR factorization that can directly compute the mixed-precision low-rank approximation of a matrix A such that the condition in equation (1) is satisfied. We make the following contributions:

1. We present, in [Section 3](#), a rounding error analysis of the Householder QR factorization where the arithmetic precision is gradually reduced in the course of the algorithm. We produce a theoretical upper bound on the error demonstrating that, if these changes of precision are appropriately operated, the accuracy of the resulting low-rank approximation can be made the same as in the case where only high-precision arithmetic is used.
2. We present, in [Section 4](#) two mixed-precision QR factorization algorithms that rely, respectively, on the Businger-Golub and randomized pivoting.
3. Finally, in [Section 5](#), we present an experimental evaluation of these algorithms which validates the theoretical findings and demonstrates the higher performance of the mixed-precision algorithms with respect to their full high-precision counterparts.

A mixed-precision algorithm for computing a mixed-precision low-rank approximation of a matrix A was recently proposed by Connolly, Higham, and Pranesh [5]. This, however, relies on the randomized range finder method [18] and the resulting low-rank approximation is stored in high precision despite the computations being carried in mixed-precision.

2 Background

In the remainder of this document, we will use the following notation. Upper-case and lower-case roman letters denote, respectively, matrices and vectors,

while Greek letters denote scalars. Subscripts will be used to denote matrix or vector indices and superscripts to denote data associated with different steps of some algorithm or sequence of operations. To keep the notation simple, when there is no ambiguity, we will denote a column of a matrix using the corresponding lower-case letter with a subscript indicating the column index; for example, the j -th column of matrix A will be denoted a_j .

2.1 Householder QR and error analysis

The Householder [15] QR factorization of an $m \times n$ matrix A proceeds in n steps where, at each step k , an elementary reflector H^k is computed such that all the subdiagonal coefficients in column k are annihilated; as a result, the A matrix is reduced into an upper triangular matrix R and the product of the reflectors defines the orthogonal Q factor:

$$H^n \cdots H^1 A = Q^T A = R, \text{ where } H^k = (I - \tau^k v^k (v^k)^T).$$

Here the Q matrix is never explicitly computed but implicitly represented by the v^k vectors and τ^k scalars; furthermore, the first $k - 1$ coefficients in vector v^k are null. The v^k and τ^k vectors can be computed in different ways, for example, to prevent cancellations; we refer the reader to the article by Lehoucq [17] for an exhaustive discussion of this argument. Our work relies on the error analysis of Higham [14] (Chapter 19) which assumes that these are computed following the convention used in the LINPACK and LAPACK libraries.

It must be noted that, for the sake of performance, these Householder transformations are not computed and applied to A individually but, rather, in blocks of size $b \ll n$ using the WY representation of Schreiber and Van Loan [21]; this allows for using Level-3 BLAS operations for most of the computations which results in a much faster execution due to an efficient use of cache memories.

In our error analysis of Section 3 we will make extensive use of the results in lemmas 19.1, 19.2 and 19.3 and theorem 19.4 of Higham [14] which we will report below (with some slight adaptations and notation changes) for the sake of self-completeness prior to extending them to the case where the factorization is truncated and conducted using multiple precisions. Accordingly, we use the standard model of floating-point arithmetic [14, sect. 2.2], we put a hat on variables to denote that they represent computed quantities. For any integer k , we define

$$\gamma_k = \frac{ku}{1 - ku}$$

where u denotes the unit rounding of the employed arithmetic; a superscript on γ denotes that u carries that superscript; thus $\gamma_k^f = \frac{ku^f}{(1 - ku^f)}$, for example. We also use the notation $\tilde{\gamma}_k = \gamma_{\eta k}$ to hide modest constants η .

Lemma 2.1 (19.1 and 19.2 of [14]). *Assume a Householder transformation H is computed and applied to a vector b using precision u . The computed result \hat{y} satisfies*

$$\hat{y} = (H + \Delta H)b, \quad \|\Delta H\|_F \leq \tilde{\gamma}_m.$$

The previous lemma demonstrates that computing and applying a Householder transformation in finite precision is a backward stable operation. The next one demonstrates that this property also holds when multiple transformations of this type are applied to a vector.

Lemma 2.2 (19.3 of [14]). *Consider the sequence of transformations*

$$b^i = H^i b^{i-1}, \quad b^0 = b, \quad i = 1, \dots, k.$$

The computed \widehat{b}^k satisfies

$$\widehat{b}^k = H^k \dots H^1 (b + \Delta b) = Q^T (b + \Delta b), \quad \|\Delta b\|_2 \leq \tilde{\gamma}_{mk} \|b\|_2.$$

A Householder QR factorization simply consists in applying to a matrix A a sequence of transformations that annihilate all the subdiagonal coefficients one column at a time; therefore, Lemma 2.2 applies on all columns, which leads to the following theorem.

Theorem 2.3 (19.4 of [14]). *Let $\widehat{R} \in \mathbb{R}^{m \times n}$ be the computed upper trapezoidal QR factor of $A \in \mathbb{R}^{m \times n}$ ($m \geq n$) obtained via the Householder QR algorithm. Then there exists an orthogonal $Q \in \mathbb{R}^{m \times m}$ such that*

$$A + \Delta A = Q \widehat{R}$$

where

$$\|\Delta a_j\|_2 \leq \tilde{\gamma}_{mn} \|a_j\|_2, \quad j = 1, \dots, n.$$

The latter theorem simply says that one such Q matrix exists. In practice, it is more useful to have a bound using the actually computed \widehat{Q} , as stated in the next Theorem.

Theorem 2.4 (from [14]). *Let $\widehat{R} \in \mathbb{R}^{m \times n}$ and $\widehat{Q} \in \mathbb{R}^{m \times m}$ be, respectively, the computed upper trapezoidal and orthogonal QR factors of $A \in \mathbb{R}^{m \times n}$ ($m \geq n$) obtained via the Householder QR algorithm. Then*

$$\|A - \widehat{Q} \widehat{R}\|_F \leq \sqrt{n} \tilde{\gamma}_{mn} \|A\|_F. \quad (2)$$

Proof. It must be noted that \widehat{Q} is obtained by applying the sequence of transformations to the identity matrix; therefore, Theorem 19.4 can be used to derive the following bound

$$\widehat{Q} = Q(I + \Delta I), \quad \|\Delta i_j\|_2 \leq \tilde{\gamma}_{mn}$$

where Δi_j denoted the j -th column of matrix ΔI ; this implies

$$\|Q - \widehat{Q}\|_F \leq \sqrt{n} \tilde{\gamma}_{mn}. \quad (3)$$

Now, using equation (3) and Theorem 2.3

$$\begin{aligned} \left\| (A - \widehat{Q} \widehat{R})_j \right\|_2 &= \left\| (A - Q \widehat{R})_j + ((Q - \widehat{Q}) \widehat{R})_j \right\|_2 \\ &\leq \tilde{\gamma}_{mn} \|a_j\|_2 + \sqrt{n} \tilde{\gamma}_{mn} \|\widehat{r}_j\|_2 \\ &= \tilde{\gamma}_{mn} \|a_j\|_2 + \sqrt{n} \tilde{\gamma}_{mn} \|Q \widehat{r}_j\|_2 \\ &= \tilde{\gamma}_{mn} \|a_j\|_2 + \sqrt{n} \tilde{\gamma}_{mn} \|a_j + \Delta a_j\|_2 \\ &= \sqrt{n} \tilde{\gamma}_{mn} \|a_j\|_2 \end{aligned}$$

which implies the result. □

2.2 QR factorization with Businger-Golub pivoting

A QR factorization capable of revealing the rank of a matrix (RRQR for Rank-Revealing QR) can be obtained using column pivoting as in the method proposed by Businger and Golub [3]. Essentially, at each step k of the QR factorization, this method permutes the columns of the trailing submatrix such that the pivotal column k is the one that has maximum 2-norm. This implies that the diagonal coefficients of the R factor are of decreasing absolute value and that the following property holds:

$$AP = QR \text{ where } |R_{k,k}| \geq \|R_{k:m,j}\|_2 \quad j = k, \dots, n. \quad (4)$$

Note that explicitly recomputing the norm of all the columns in the trailing submatrix not only is expensive but completely prevents the use of blocking (and, thus, of Level-3 BLAS operations) because this requires to entirely update all the remaining columns after every elimination step. This problem can be partially overcome taking advantage of the fact that, once all the column norms of the original A matrix have been computed, these do not have to be recomputed at every step but can be cheaply updated. Essentially, at step k of the factorization, the norm of column j in the trailing submatrix is updated by subtracting the freshly computed $R_{k,j}$ coefficient. This approach is shown in Algorithm 1 which we refer to as QRCP; here we have assumed that V is a matrix containing all the computed v^k vectors in its columns, that $\text{householder}(x, k)$ is a function which computes and applies a Householder reflection that annihilates the bottom $m - k + 1$ coefficients of a vector x of size m and that W is a workspace. Although, in this algorithm, a large portion of computations is still done using Level-2 BLAS operations, some Level-3 can be used (in line 13).

Algorithm 1 Blocked QR factorization with Businger-Golub pivoting (QRCP).

```

1: Input:  $A \in \mathbb{R}^{m \times n}$ 
2: Let:  $\eta_j = \|A_{:,j}\|_2, \quad j = 1, \dots, n, \quad P = I$ 
3: for  $j = 1 : b : n$  do
4:   for  $k = j : j + b - 1$  do
5:     Find  $i \in k, \dots, n$  such that  $\eta_i$  is minimal
6:     Swap columns  $k$  and  $i$  in  $A$  and  $P$ 
7:      $A_{k:m,k} = A_{k:m,k} - V_{k:m,j:k-1}W_{j:k-1,k}$ 
8:      $v^k, \tau^k = \text{householder}(A_{:,k}, k)$ 
9:      $W_{k+1,k:n} = \tau^k (v^k)^T A_{:,k+1:n} + \tau^k (v^k)^T V_{:,j:k-1}W_{j:k-1,k+1:n}$ 
10:     $A_{k,k+1:n} = A_{k,k+1:n} - V_{k,j:k-1}W_{j:k-1,k+1:n}$ 
11:     $\eta_i = \sqrt{\eta_i^2 - A_{k,i}^2}, \quad i = k + 1, \dots, n$ 
12:   end for
13:    $A_{j+b:m,j+b:n} = A_{j+b:m,j+b:n} - V_{j+b:m,j+j+b-1}W_{j:j+b-1,j+b:n}$ 
14: end for
15: Output:  $Q = \prod_{k=1,n} (I - \tau^k v^k (v^k)^T), \quad R = \text{triu}(A), \quad P$ 

```

It must be noted that the column norm update in line 11 of Algorithm 1 is a very delicate step when carried in finite precision as it may be subject to severe cancellations. This problem might be overcome using the approach proposed by Drmač and Bujanović [8] where if, in line 11 the norm of some columns drops by a value larger than a prescribed threshold which depends on the arithmetic unit roundoff, the algorithm breaks out of the inner loop of line 4, fully updates the trailing submatrix (line 13) and explicitly recomputes the norm of the problematic columns. This approach might reduce the portion of Level-3 BLAS operations but renders the method robust. Algorithm 1 with this updating technique is implemented in the LAPACK `_GEQP3` routine.

2.3 QR factorization with randomized pivoting

In practice, Algorithm 1 achieves very poor performance and parallel scalability because a large portion of computations in Algorithm 1 are of Level-2 BLAS type and because of the numerous communications that the Businger-Golub pivoting requires. For this reason alternative pivoting techniques have been proposed in the literature that aim at overcoming these drawbacks. Multiple methods proposed in the literature, such as those by Duersch and Gu [9], Martinsson et al. [19], Demmel et al. [6], and Dessolet and Marcuzzi [7], rely on an approach where, at every step of the factorization, not one but b (the panel size) selected columns of the trailing submatrix are moved upfront, eliminated and the corresponding transformations applied at once using Level-3 BLAS operations as in the WY technique described above. These methods essentially differ in the way these b columns are selected. In the approach proposed by Duersch and Gu [9] and Martinsson et al. [19], illustrated in Algorithm 2, this selection is done using randomized sampling, that is, the trailing submatrix is left-multiplied by a i.i.d. Gaussian matrix $\Omega \in \mathcal{N}(0, 1)^{(b+p) \times (m-j)}$ which produces a sample matrix S ; here we assume that $j - 1$ columns of A have already been eliminated and p is an *oversampling* parameter of moderate value (less than ten). Because of the properties that connect S to the trailing submatrix, the “important” b columns can be selected by applying QRCP to the sample matrix S . This drastically improves the amount of level-3 BLAS operations because S has a much smaller row-dimension than the trailing submatrix. As a matter of fact, the sample matrix S does not have to be recomputed at every factorization step but it can be computed only once and cheaply updated [9, 19].

Algorithm 2 Blocked QR factorization with randomized pivoting (QRRP).

```

1: Input:  $A \in \mathbb{R}^{m \times n}$ 
2: Let:  $P = I$ ,  $\Omega \in \mathcal{N}(0, 1)^{(b+p) \times (m-j)}$ ,  $S = \Omega A$ 
3: for  $j = 1 : b : n$  do
4:    $\tilde{Q}, \tilde{R}, \tilde{P} = \text{QRCP}(S_{:,j:n})$ 
5:    $A_{:,j:n} = A_{:,j:n} \tilde{P}$ ,  $P_{:,j:n} = P_{:,j:n} \tilde{P}$ 
6:    $Q^j, R^j = \text{QR}(A_{j:m,j:j+b-1})$ 
7:    $A_{j:m,j+b:n} = (Q^j)^T A_{j:m,j+b:n}$ 
8:   Update  $S$ 
9: end for
10: Output:  $Q = \prod Q^j$ ,  $R = \text{triu}(A)$ ,  $P$ 

```

Xiao, Gu, and Langou [22] demonstrate that the property of equation (4) does not apply formally to the result of QRRP but holds in a probabilistic sense. Given ε , $\Delta \in (0, 1)$ and an oversampling parameter $p \geq \lceil \frac{4}{\varepsilon^2 - \varepsilon^3} \log(\frac{2nk}{\Delta}) \rceil$ the following property

$$|R_{k,k}| \geq \sqrt{\frac{1-\varepsilon}{1+\varepsilon}} \|R_{k:m,j}\|_2, \quad i+1 \leq j \leq n \quad (5)$$

holds with probability at least $1 - \Delta$.

3 Error analysis

Let us assume that we have p precisions such that the respective unit roundoff verify

$$u^1 \leq u^2 \leq \dots \leq u^p$$

and for each precision i a sequence of k^i transformations are computed and applied to matrix A such that

$$\sum_{i=1}^p k^i = k \leq n.$$

Therefore, first k^1 transformations are computed and applied with precision u^1 , then k^2 with precision u^2 and so forth:

$$\overbrace{(H^{p,k^p} \dots H^{p,1})}^{u_p} \dots \overbrace{(H^{1,k^1} \dots H^{1,1})}^{u_1} A = Q^T A = \begin{bmatrix} R \\ A^{p+1} \end{bmatrix}. \quad (6)$$

Here we use an extra superscript to denote the precision at which each transformation is computed and applied. furthermore, we denote A^{i+1} the trailing submatrix after K^i of the above transformations are applied where

$$K^i = \sum_{j=1}^i k^j.$$

Note that, because we are interested in a truncated QR factorization, k might be smaller than n , in which case A^{p+1} corresponds to a $(m - k) \times n$ matrix with the rightmost $n - k$ columns being non-zero.

Each A^i matrix has $m - K^{i-1}$ rows and n columns, the first K^{i-1} being equal to zero; A^1 corresponds to the initial matrix A . The Q and R matrices in equation (6) can be split in block-columns and block-rows, respectively, such that

$$A = [Q_1 \dots Q_p Q_{p+1}] \begin{bmatrix} R_1 \\ \vdots \\ R_p \\ A^{p+1} \end{bmatrix}. \quad (7)$$

Note that each Q_i is a $m \times k^i$ submatrix of Q and is the result of computations carried in precisions 1 through i . Equivalently, R_i is a $k^i \times n$ submatrix of R and is the result of computations carried in precisions 1 through i . Our mixed-precision low-rank approximation of A is obtained by dropping Q_{p+1} and A^{p+1} in the above equation.

Our analysis will rely on the observation that in the QR factorization the i -th of such transformations has the following structure

$$\begin{bmatrix} I^{i-1} & \\ & \bar{H}^i \end{bmatrix}$$

where I^{i-1} is the identity matrix of size $i-1$; this is because the i -th transformation is computed so as to annihilate all the subdiagonal coefficients in the i -th column of A and implies that the application of such transformation will only concern the bottom $m - i + 1$ rows of the matrix. In the analysis of Higham [14] this property was not used because in the case where a single precision is used it does not yield any significant improvement of the bounds. For our analysis, it is not necessary to consider the structure of each single transformation but, rather, it is enough to note that all transformations at precision i have the same structure

$$\begin{bmatrix} I^{K^{i-1}} & \\ & \bar{H}^{i,j} \end{bmatrix}, \quad j = 1, \dots, k^i.$$

Lemma 3.1 (equivalent of Lemma 2.2 in mixed precision). *Consider the sequence of transformations*

$$b^{K^i} = \prod_{j=1}^{k^i} H^{i,j} b^{K^{i-1}}, \quad b^0 = b, \quad i = 1, \dots, p, \quad K^p = k.$$

where all transformations $H^{i,j}$, $j = 1, \dots, k^i$ are computed and applied in precision u^i and have the following structure

$$H^{i,j} = \begin{bmatrix} I^{K^{i-1}} & \\ & \bar{H}^{i,j} \end{bmatrix}. \quad (8)$$

The computed \hat{b}^k satisfies

$$\hat{b}^k = Q^T(b + \Delta b), \quad \|\Delta b\|_2 \leq \sum_{i=1}^p \tilde{\gamma}_{mk^i}^i \|b_{K^{i-1}+1:m}^{K^{i-1}}\|_2.$$

Proof. The results follows by using Theorem 2.2 “in packets” where, in each packet, the Householder transformations have the structure of equation (8). Each packet of k^i transformation at precision u^i only concerns rows $K^{i-1}+1, \dots, m$ of $b^{K^{i-1}}$ and, by Theorem 2.2, introduces an error bounded by $\tilde{\gamma}_{mk^i}^i \|b_{K^{i-1}+1:m}^{K^{i-1}}\|_2$. Note that it would be more appropriate to use $\tilde{\gamma}_{(m-K^{i-1})k^i}^i$ but we use m instead of $m - K^{i-1}$ to keep the notation simple. \square

Based on Lemma 3.1, we are now ready to derive a columnwise error bound for a truncated QR factorization in mixed precision.

Lemma 3.2 (equivalent of Lemma 2.3 with truncation and mixed precision). *Assume that a truncated QR factorization is computed such that $k \leq n$ Householder transformations are computed and applied to a matrix $A \in \mathbb{R}^{m \times n}$ using p different precisions of increasing unit roundoff u^i . Let k^i be the number of transformations that are computed using precision u^i . Then there exist matrices Q_1, \dots, Q_{p+1} such that the computed \hat{R}^i and \hat{A}^{p+1} satisfy*

$$(A + \Delta A) = [Q_1 \cdots Q_p Q_{p+1}] \begin{bmatrix} \hat{R}_1 \\ \vdots \\ \hat{R}_p \\ \hat{A}^{p+1} \end{bmatrix}, \quad \|\Delta a_j\|_2 \leq \sum_{i=1}^p \tilde{\gamma}_{mk^i}^i \|a_j^i\|_2 \quad (9)$$

and, consequently,

$$\left\| \left(A - \sum_{i=1}^p Q_i \hat{R}_i \right)_j \right\|_2 \leq \|a_j^{p+1}\|_2 + \sum_{i=1}^p \tilde{\gamma}_{mk^i}^i \|a_j^i\|_2. \quad (10)$$

Proof. Equation (9) straightforwardly results from the application of Lemma 3.1 to the case where the sequence of Householder transformations is computed so as to annihilate all the subdiagonal coefficients of A and, therefore, have the structure defined in equation (8). Equation (10), instead, follows from the observation that

$$\hat{a}_j^{p+1} = a_j^{p+1} + \Delta a_j^{p+1}, \quad \|\Delta a_j^{p+1}\|_2 \leq \sum_{i=1}^p \tilde{\gamma}_{mk^i}^i \|a_j^i\|_2.$$

□

Theorem 3.3 (equivalent of Theorem 2.4 with truncation and mixed precision). *Assume that a truncated QR factorization is computed such that $k \leq n$ Householder transformations are computed and applied to a matrix $A \in \mathbb{R}^{m \times n}$ using p different precisions of increasing unit roundoff u^i . Let k^i be the number of transformations that are computed using precision i . The computed \hat{R}_i and \hat{Q}_i satisfy*

$$\left\| A - \sum_{i=1}^p \hat{Q}_i \hat{R}_i \right\|_F \leq \|A^{p+1}\|_F + \sum_{i=1}^p \sqrt{k^i} \tilde{\gamma}_{mk^i}^i \|A^i\|_F. \quad (11)$$

Proof. Following the same path that led us to equation (3), in the case where multiple precisions are used we obtain

$$\|Q_i - \hat{Q}_i\|_F \leq \sqrt{k^i} \sum_{j=1}^i \tilde{\gamma}_{mk^j}^j = \sqrt{k^i} \tilde{\gamma}_{mk^i}^i$$

which allows us to derive a bound on the quality of the approximation using the actually computed \hat{Q}_i and \hat{R}_i

$$\begin{aligned} \left\| \left(A - \sum_{i=1}^p \hat{Q}_i \hat{R}_i \right)_j \right\|_2 &= \left\| \left(A - \sum_{i=1}^p Q_i \hat{R}_i \right)_j + \sum_{i=1}^p \left((Q_i - \hat{Q}_i) \hat{R}_i \right)_j \right\|_2 \\ &\leq \left\| \left(A - \sum_{i=1}^p Q_i \hat{R}_i \right)_j \right\|_2 + \sum_{i=1}^p \|Q_i - \hat{Q}_i\|_F \left\| \left(\hat{R}_i \right)_j \right\|_2 \\ &\leq \|a_j^{p+1}\|_2 + \sum_{i=1}^p \tilde{\gamma}_{mk^i}^i \|a_j^i\|_2 + \sum_{i=1}^p \sqrt{k^i} \tilde{\gamma}_{mk^i}^i \left\| \left(\hat{R}_i \right)_j \right\|_2 \\ &\leq \|a_j^{p+1}\|_2 + \sum_{i=1}^p \sqrt{k^i} \tilde{\gamma}_{mk^i}^i \|a_j^i\|_2 \end{aligned}$$

which implies the result. □

4 Pivoted QR factorization in mixed precision

Based on the theoretical findings of the previous section, we are now ready to formulate a truncated rank-revealing QR factorization in mixed precision. We will first introduce two truncated QR factorization algorithms based, respectively, on the Businger-Golub and randomized pivoting and then a mixed-precision algorithm that can use either of these.

Specifically, the truncated mixed-precision algorithm relies on the use of the error bound in equation (11) to gradually switch to lower precision and, eventually, to halt the factorization as soon as the prescribed accuracy ε is reached. The terms of this bound, however, are difficult, in practice, to compute accurately. In order to make this bound more usable in practice, we can proceed to some simplifications. First of all we can ignore the constants related to the accumulation of rounding errors, which are often pessimistic [13]; this amounts to replacing each $\tilde{\gamma}_{mk^i}^i$ with the unit roundoff of the corresponding arithmetic precision u^i . Second, because in the course of the factorization it is not known beforehand how many transformations will be computed with each precision i , we will replace k^i with $n - K^{i-1}$. The error bound thus becomes

$$\left\| A - \sum_{i=1}^p \widehat{Q}_i \widehat{R}_i \right\|_F \leq \|A^{p+1}\|_F + \sum_{i=1}^p \sqrt{n - K^{i-1} u^i} \|A^i\|_F. \quad (12)$$

Assuming that a low-rank approximation of relative accuracy ε is to be computed

$$\left\| A - \sum_{i=1}^p \widehat{Q}_i \widehat{R}_i \right\|_F \leq \|A^{p+1}\|_F + \sum_{i=1}^p \sqrt{n - K^{i-1} u^i} \|A^i\|_F \leq \varepsilon \|A\|_F$$

and, once again, ignoring the constants, it will be enough to ensure that all the terms in the bound are smaller than or equal to $\varepsilon \|A\|_F$. That is to say, it will be possible to switch from precision i to precision $i + 1$ at step j of the factorization such that

$$\sqrt{n - j u^{i+1}} \|A_{j:m, j:n}\|_F \leq \varepsilon \|A\|_F \quad (13)$$

and the factorization can be truncated at step k such that

$$\|A_{k:m, k:n}\|_F \leq \varepsilon \|A\|_F. \quad (14)$$

It must be noted that our error analysis does not make any assumption on how the pivoting is done. Actually, for our method to work, it is only required that the norm of the trailing submatrix decreases in the course of the factorization which happens even in the case where no pivoting is applied. Obviously, the use of pivoting will lead to a faster decay of the trailing submatrix norm and, consequently, to an earlier truncation and change of precisions.

4.1 Truncated QR factorization with Businger-Golub pivoting

The two criteria in equations (13) and (14) can be straightforwardly used used to halt Algorithm 1 because the Frobenius norm of the trailing submatrix is readily available as the 2-norm of part of the vector storing the η_i , that is, the 2-norm of the corresponding columns. The resulting algorithm is presented in Algorithm 3 and amounts to a simple modification of Algorithm 1 where the factorization is interrupted as soon as either equation (13) or (14) is verified. It must be noted that, when the truncation happens because equation (13) is verified, it is implicitly assumed that the factorization will be continued using a lower precision (see the details in Section 4.3) and, therefore, the trailing submatrix update on line 17 is necessary. If, instead, the factorization is interrupted because equation (14) is verified, the trailing submatrix is discarded and therefore need not be updated; for the sake of conciseness we do not include this optimization in Algorithm 3 although it is implemented in the code we used for the experimental evaluation of Section 5.2.

It must be noted that, thanks to the property in equation (4), the Frobenius norm of the trailing submatrix at step k can be bounded using $|R_{k,k}|$, that is, $\|A_{k:n, k:n}\|_F \leq \sqrt{n - k} |R_{k,k}|$; this criterion, however, can largely overestimate the norm of the trailing submatrix and result in a late switch of precision, or truncation leading to sub-optimal performance.

4.2 Truncated QR factorization with randomized pivoting

In the case of the QR factorization with randomized pivoting in Algorithm 2, the norm of the trailing submatrix cannot be easily computed. Nevertheless, it is possible to check for precision switch and truncation within the QRCP factorization of the sample matrix based on the norm of the trailing submatrix of the

Algorithm 3 Truncated blocked QR factorization with Businger-Golub pivoting (TQRCP).

```

1: Input:  $A \in \mathbb{R}^{m \times n}$ ,  $\varepsilon_t$ ,  $\varepsilon_p$ 
2: Let:  $\eta_j = \|A_{:,j}\|_2$ ,  $j = 1, \dots, n$ ,  $P = I$ 
3: for  $j = 1 : b : n$  do
4:   for  $k = j : j + b - 1$  do
5:     if  $\|\eta_{k:n}\|_2 \leq \varepsilon_t$  or  $\sqrt{n-j} \|\eta_{k:n}\|_2 \leq \varepsilon_p$  then
6:        $b = k - j$ ;  $k = k - 1$ 
7:       goto 17 and break
8:     end if
9:      $\arg \min_i \{\eta_i, i = k : n\}$ 
10:    Swap column  $k$  and  $i$  in  $A$  and  $P$ 
11:     $A_{k:m,k} = V_{k:m,j:k-1} W_{j:k-1,k}$ 
12:     $v^k, \tau^k = \text{householder}(A_{:,k})$ 
13:     $W_{k+1,k:n} = \tau^k (v^k)^T A_{:,k+1:n} + \tau^k (v^k)^T V_{:,j:k-1} W_{j:k-1,k+1:n}$ 
14:     $A_{k,k+1:n} = A_{k,k+1:n} - V_{k,j:k-1} W_{j:k-1,k+1:n}$ 
15:     $\eta_i = \sqrt{\eta_i^2 - A_{k,i}^2}$ ,  $i = k + 1, \dots, n$ 
16:   end for
17:    $A_{j+b:m,j+b:n} = V_{j+b:m,j+j+b-1} W_{j+j+b-1:j+b:n}$ 
18: end for
19: Output:  $Q_{1:m,1:k} = \prod_{i=1,k} (I - \tau^i v^i (v^i)^T)$ ,  $R = \text{triu}(A_{1:k,1:n})$ ,  $P$ ,  $k$ 

```

sample. According to Theorem 3.1 by Duersch and Gu [9], after i transformations the trailing 2-norm squared of the sample, that is, the norm of the columns in the trailing submatrix of the sample, can be written as a factor of the actual trailing column norms. Assuming S is a sample of row-dimension $l = b + p$ for a matrix A and S^i and A^i the corresponding trailing submatrices after i Householder transformations, $\|s_j^i\|_2^2 = x_j \|a_j^i\|_2^2$ where x_j has a truncated chi-squared distribution with $l - i$ degrees of freedom. Although the expectation of x_j can theoretically be smaller than $l - i$, in practice we have found that assuming $x_j = l - i$ or, more conservatively, $x_j = p$ works very well on our experimental test set (see experiments in Section 5.2). Alternatively, the property in equation (5) can be used to obtain a probabilistic bound on the norm of the trailing submatrix but this would likely result in an excessively pessimistic criterion.

Based on this discussion, we propose the truncated QR factorization with randomized pivoting in Algorithm 4; this relies on Algorithm 3 for the factorization of the sample matrix.

4.3 Truncated QR factorization in mixed precision

The truncated QR factorization in mixed precision is illustrated in Algorithm 5. Essentially, assuming p precisions are to be used, the algorithm proceeds in p iterations where, at iteration i , the current trailing submatrix A^i is factorized in precision u^i using either Algorithm 3 or 4 and, then, the resulting trailing submatrix A^{i+1} is cast into precision u^{i+1} .

5 Numerical experiments

In this section we present an experimental evaluation of the theoretical results and algorithms presented in the previous sections. This evaluation is twofold. First, in Section 5.1 we validate the correctness of the error analysis in Sec-

Algorithm 4 Truncated blocked QR factorization with randomized pivoting (TQRRP).

```

1: Input:  $A \in \mathbb{R}^{m \times n}$ ,  $\varepsilon_t$ ,  $\varepsilon_p$ 
2: Let:  $P = I$ ,  $\Omega \in \mathcal{N}(0, 1)^{(b+p) \times (m-j)}$ ,  $S = \Omega A$ 
3: for  $j = 1 : b : n$  do
4:    $\tilde{Q}, \tilde{R}, \tilde{P}, \tilde{k} = \text{TQRCP}(S_{:,j:n}, \sqrt{p}\varepsilon_t, \sqrt{p}\varepsilon_p)$ 
5:    $A_{:,j:n} = A_{:,j:n}\tilde{P}$ ,  $P_{:,j:n} = P_{:,j:n}\tilde{P}$ 
6:    $Q^j, R^j = \text{QR}(A_{j:m,j+j\tilde{k}-1})$ 
7:    $A_{j:m,j+j\tilde{k}:n} = (Q^j)^T A_{j:m,j+j\tilde{k}:n}$ 
8:   if  $\tilde{k} \leq b$  then
9:     break
10:  end if
11:  Update  $S$ 
12: end for
13: Output:  $Q_{:,1:k} = \prod Q^j$ ,  $R = \text{triu}(A_{1:k,1:n})$ ,  $P$ ,  $k = j + \tilde{k}$ 

```

Algorithm 5 Truncated RRQR factorization in mixed precision (MPTRRQR).

```

1: Input:  $A \in \mathbb{R}^{m \times n}$ ,  $\varepsilon$ ,  $[u^1, \dots, u^p]$ 
2: Let:  $A^1 = A$ ,  $u^{p+1} = \infty$ 
3: for  $i = 1, \dots, p$  do
4:   Set working precision to  $u^i$ 
5:    $Q^i, R^i, P^i, k^i = \text{TQR*P}(A^i, \varepsilon \|A\|_F, \varepsilon \|A\|_F / u^{i+1})$ 
6:   if  $i < p$ ,  $A^{i+1} = \text{cast}(A_{k^i+1:,k^i+1:}^i, u^{i+1})$ 
7: end for

```

tion 3 using up to three different precisions, that is, double (fp64), single (fp32) and BFloat16 (bf16). Second, in Section 5.2, we assess the performance of the mixed-precision variants compared with their high-precision counterpart; for these experiments, we will use precisions for which support is available in commodity CPUs and optimized LAPACK and BLAS libraries, namely double and single precision.

Experiments were conducted on the following problems:

- **randsvd** [14]: random matrices with geometrically distributed singular values between 1 and 10^{-16} ;
- **gravity** [12]: Discretization of a 1-D model problem in gravity surveying;
- **heat** [12]: inverse heat equation;
- **kahan** [16]: this is a triangular matrix with columns of decreasing norms; therefore, the pivoted QR factorization does not perform any computations. To avoid this trivial behavior, we scaled the columns of this matrix in such a way that column j is multiplied by $(1 - \tau)^{n-j}$ with $\tau = 10^{-10}$ and n being the number of columns in the matrix;
- **phillips** [12]: Phillips' famous test problem;

for all problems, only square matrices were generated of varying sizes.

5.1 Theory validation with a Julia prototype

In this section we present an experimental analysis aiming at validating the theoretical analysis of Section 3. For this purpose, we have implemented a

prototype using the Julia language which provides half precision, namely, the BFloat16 arithmetic through the BFloat16s¹ package. Because the only purpose of this prototype is to validate the theoretical results, it does not actually implement Algorithms 3 and 4 but, instead, proceeds through the following steps:

1. Fully factorizes the input matrix A using Householder QR with Businger-Golub pivoting (i.e., Algorithm 1);
2. explicitly permutes the input matrix $\tilde{A} = AP$ using the permutation resulting from the previous step;
3. computes the k^i based on criteria in equations (13) and (14) using, instead of A , the R factor resulting from step 1;
4. factorizes \tilde{A} using Algorithm 5 with standard, unpivoted QR on line 5.

Note that this procedure is consistent with the fact that our error analysis does not make any assumptions on whether and how the pivoting is done, as explained in Section 4.

Tables 1 and 2 show experimental results for the randsvd and phillips matrices, respectively, of size 2048. In the first column we report the value of the chosen ε threshold, in the second, the measured error when the factorization is computed entirely in double precision, in the third the error bound computed using equation (12) assuming three precisions are used, in the fourth the actual error and in the fifth, sixth and seventh, respectively, the column at which happened the precision switch from fp64 to fp32, the precision switch from fp32 to bf16 and the truncation; note that the truncation happens on the same column both in full double precision and mixed precision. The following conclusions can be drawn by these results. First, the error bound slightly exceeds but closely tracks the ε threshold; this is perfectly expected because in our error analysis some constants were ignored. Second, the actual error never exceeds the bound, which validates our rounding error analysis. Third, as the ε threshold grows, an increasingly large amount of factorization steps are computed using lower-precision arithmetics; clearly, as ε exceeds $u_s\sqrt{n}$, fp64 is not needed anymore and all computations are done in fp32 and bf16. All these observations are confirmed by experiments conducted on the other matrices of our test set which we omit for the sake of space.

	fp64	fp64/fp32/bf16				
ε	Error	Bound	Error	fp64/fp32	fp32/bf16	Trunc.
1.0e-14	9.80e-15	3.42e-14	1.04e-14	1184	1781	1898
1.0e-12	9.72e-13	2.40e-12	1.04e-12	929	1538	1637
1.0e-10	9.79e-11	2.27e-10	1.02e-10	670	1287	1375
1.0e-08	9.75e-09	2.18e-08	1.03e-08	404	1033	1112
1.0e-06	9.78e-07	2.17e-06	1.02e-06	125	775	850
1.0e-05	9.75e-06	1.81e-05	1.02e-05	1	645	717
1.0e-04	9.73e-05	1.53e-04	1.01e-04	1	514	584
1.0e-03	9.74e-04	1.51e-03	1.02e-03	1	379	448
1.0e-02	9.75e-03	1.53e-02	1.02e-02	1	243	310

Table 1: Error and use of precisions for the randsvd matrix of size 2048.

In Figure 1 we report results of an image compression experiment for an image of size 1057×1600 . In this figure we compare the original image (*top-left*) with images that are compressed using a truncated QR factorization in full

¹<https://github.com/JuliaMath/BFloat16s.jl>

	fp64	fp64/fp32/bf16				
ε	Error	Bound	Error	fp64/fp32	fp32/bf16	Trunc.
1.0e-14	1.20e-15	2.44e-13	8.36e-14	1850	2048	2049
1.0e-12	1.20e-15	2.02e-12	6.50e-13	775	2046	2049
1.0e-10	4.07e-11	2.76e-10	5.54e-11	141	1989	2047
1.0e-08	9.92e-09	2.75e-08	1.13e-08	25	1267	1749
1.0e-06	9.93e-07	2.89e-06	1.05e-06	7	291	442
1.0e-05	9.83e-06	2.59e-05	1.02e-05	1	117	188
1.0e-04	9.55e-05	2.14e-04	1.05e-04	1	51	76
1.0e-03	9.12e-04	2.33e-03	1.11e-03	1	22	31
1.0e-02	7.62e-03	2.20e-02	1.19e-02	1	11	15

Table 2: Error and use of precisions for the phillips matrix of size 2048.

fp32 (*top-right*), fp32/bf16 (*bottom-left*) and full bf16 (*bottom-right*) and then reconstructed in fp32. Here, the truncation threshold ε was set to 0.04 and thus only fp32 and bf16 arithmetics were used; the truncation happened on column 191 in all the three reconstructed images. It can clearly be seen that using bf16 only it is not possible to achieve a satisfactory compression. Both the other two approaches, instead, achieve a satisfactory result although, in the mixed-precision case, only 12 out of 190 columns are computed and stored in fp32 and the rest in bf16 which might result in considerable time savings especially on modern GPUs where bf16 computations are much faster than fp32 ones.

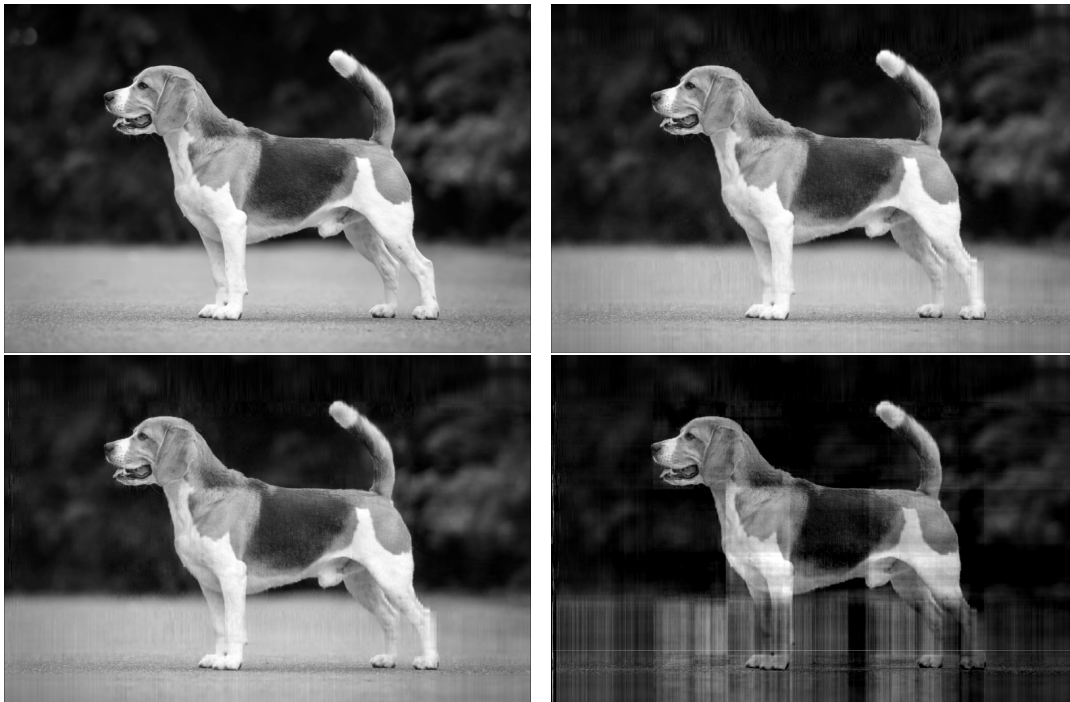


Figure 1: Image compression. Original image (*top-left*); reconstructed image after compression in full fp32 (*top-right*), in fp32/bf16 (*bottom-left*) and full bf16 (*bottom-right*). ε was set to 0.04 and the truncation happened at column 190 but in the mixed-precision case only 12 transformations were computed in fp32 and the rest in bf16. Image size is 1057×1600 .

5.2 Performance analysis with optimized code

In this section we evaluate the performance improvement brought by the use of the mixed-precision algorithm proposed in Section 4.3 using both Businger-Golub and randomized pivoting compared with the full, high-precision corresponding variants. For these experiments we have implemented Algorithms 3, 4 and 5 in the Fortran language. The code for Algorithm 3 is a straightforward adaptation of the DGEQP3/SGEQP3 and DLAQPS/SLAQPS routines in LAPACK. Algorithm 4, instead, is implemented with an entirely new code which, however, heavily relies on other LAPACK and BLAS routines.

Our experiments were conducted on an AMD Zen3 EPYC 7763 processor, using the BLAS and LAPACK routines in the Intel MKL 2020 package and the GNU gfortran 11.2 Fortran compiler. All experiments are sequential; although parallelism could be straightforwardly used within BLAS operations, we have chosen not to do so because this does not bring any specific insight on the behavior of the proposed methods.

Figure 2 shows, for the matrices in our test set, the execution time for double-precision (dark color) and mixed single/double-precision (light color) truncated QR factorization algorithms with Businger-Golub (yellow) and randomized (blue) pivoting with respect to the truncation threshold ε . For each matrix, the values are normalized to the execution time of the corresponding full double-precision QR factorization.

The behavior of the proposed algorithms varies considerably across the test problems. Nevertheless, some conclusions can be drawn.

Obviously, the benefit of using the mixed-precision algorithms heavily depends on the spectrum of the problem and the distribution of its singular values which ultimately determines the ratio of operations that are done in double and single precision. As the truncation threshold increases, this ratio normally evolves favorably making the potential benefit of mixed precision higher. This is clearly visible on the randsvd matrix. Although this trend also applies to the other matrices, the execution time does not always evolve correspondingly. This is due to the fact that the ratio of double and single-precision operations alone does not entirely describe performance but other factors must be taken into account. One important factor is the arithmetic intensity of operations. Despite the fact that a fixed panel size is chosen for all algorithms, as explained in Section 2.2, a panel reduction may be interrupted if the norm of some columns drops beyond a prescribed value which eventually reduces the granularity of operations and, consequently, their speed. This happens in a hardly predictable way and may adversely affect the speed of computation in either double or single precision. This behavior is clearly visible on the phillips matrix comparing the results obtained on the Businger-Golub case with $\varepsilon = 10^{-12}$ and $\varepsilon = 10^{-8}$: in the second case, the single to double-precision operations ratio is more favorable but a large number of restarts happens during the single-precision computations. As a result, the mixed-precision algorithm is slightly slower than the double-precision one, whereas, in the first case, it is 33% faster. Note that in the variant with randomized pivoting, restarts happen in the pivoted factorization of the sample matrix; however, this operation only accounts for a small fraction of the overall operational complexity and, therefore, these restarts have a limited impact. Note that, on standard CPUs, single-precision computations are expected to be twice as fast as double-precision ones. For CPU-bound operations, this is mainly related to the use of vector units (one vector instruction can do twice as many fp32 operations as fp64 ones) whereas for memory-bound operations this is due to a better use of the memory bandwidth (twice as many fp32 coefficients can be transferred as fp64 in the same time). Nevertheless, this assumption does not

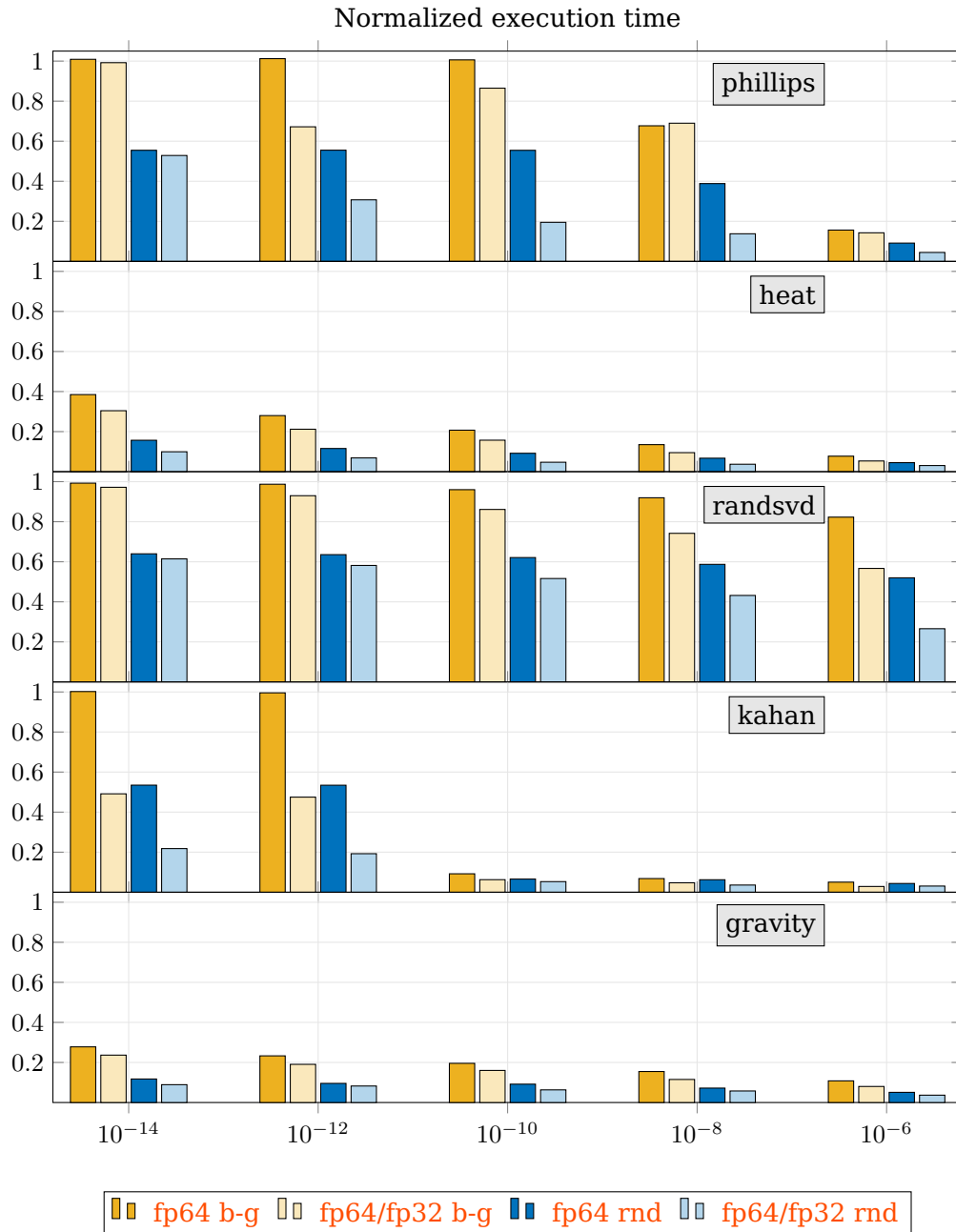


Figure 2: Execution times for double-precision (dark color) and mixed single/double-precision (light color) truncated QR factorization algorithms with Businger-Golub (yellow) and randomized (blue) pivoting with respect to the truncation threshold ε . All values are normalized to the execution time of the full double-precision QR factorization. All the matrices are of size 8192.

take into account other factors related to the use of cache memories. Although we cannot assume that the original matrix fits into cache, at some point of the factorization the trailing submatrix, whose size is smaller and smaller, will; when single precision is used, this will happen at an earlier step of the factorization with respect to the double-precision case. Although we haven't conducted dedicated experiments to validate this effect, we speculate that it can explain the fact that in some cases the mixed-precision algorithm is more than twice as fast

as the full double-precision one (for example the randomized algorithm on the phillips matrix at $\varepsilon = 10^{-10}$ or the kahan matrix at $\varepsilon = 10^{-12}$).

6 Conclusions and future work

In this work we have introduced a mixed-precision truncated Householder QR factorization where the arithmetic precision of computations is gradually reduced as the norm of the trailing submatrix decreases. We presented an error analysis that results in an error bound demonstrating that if these changes of precision are appropriately operated, the resulting mixed-precision low-rank representation has the same accuracy as in the case where all computations are done in high precision.

Based on our theoretical findings, we have presented two Householder QR factorization algorithms based on Businger-Golub and randomized pivoting, respectively. Pivoting is not necessary for the mixed-precision algorithm to work because this simply relies on the assumption that the Frobenius norm of the trailing submatrix decreases, which holds true regardless of pivoting; nevertheless, if pivoting is applied, the trailing submatrix norm decays much faster which ultimately leads to more compact low-rank representations and more efficient use of low-precision arithmetics.

We have presented a twofold experimental analysis. First we focused on validating the theoretical analysis. We did this using a prototype written in the Julia language where we could use up to three different precisions. The corresponding experiments validate the presented theoretical analysis. Second, we evaluated the performance of the two proposed mixed-precision algorithms using double and single-precision arithmetics. Our experimental results on synthetic matrices with different spectra demonstrate that the mixed-precision algorithms can achieve better performance than the full double-precision counterparts, sometimes exceeding a factor two.

Some opportunities can be identified for pushing the presented ideas further. First, the performance of the mixed-precision algorithms must be evaluated using even lower-precision arithmetic such as Float16 or BFloat16 which, on some hardware, achieve much higher performance than single precision; these are supported in hardware on modern CPUs and GPUs but the corresponding LAPACK and BLAS libraries are still lacking, which prevents us from implementing the mixed-precision algorithms. Second, we must investigate whether and how our approach can be used with other pivoting strategies such as tournament pivoting which might be better suited to parallel implementations. Finally, we would like to study scaling algorithms to prevent issues related to overflow and underflow in low-precision computations.

7 Acknowledgments

This work was supported by the France 2030 NumPEX Exa-Soft (ANR-22-EXNU-0003) project managed by the French National Research Agency (ANR) and the ANR MixHPC project (ANR-23-CE46-0005-01).

Experiments presented in this paper were carried out using the PlaFRIM experimental testbed, supported by Inria, CNRS (LABRI and IMB), Université de Bordeaux, Bordeaux INP and Conseil Régional d'Aquitaine ².

²<https://www.plafrim.fr>

André Pachteau was supported by the National Polytechnic Institute of Toulouse (Toulouse INP) through the EIT program.

References

- [1] Patrick Amestoy et al. “Mixed precision low-rank approximations and their application to block low-rank LU factorization”. In: *IMA Journal of Numerical Analysis* (Aug. 2022). drac037. ISSN: 0272-4979. DOI: [10.1093/imanum/drac037](https://doi.org/10.1093/imanum/drac037).
- [2] Patrick Amestoy et al. “On the Complexity of the Block Low-Rank Multifrontal Factorization”. In: *SIAM Journal on Scientific Computing* 39.4 (2017), A1710–A1740. DOI: [10.1137/16M1077192](https://doi.org/10.1137/16M1077192).
- [3] Peter Businger and Gene H. Golub. “Linear Least Squares Solutions by Householder Transformations”. In: *Numer. Math.* 7.3 (June 1965), pp. 269–276. ISSN: 0029-599X. DOI: [10.1007/BF01436084](https://doi.org/10.1007/BF01436084).
- [4] Tony F. Chan. “Rank revealing QR factorizations”. In: *Linear Algebra and its Applications* 88-89 (1987), pp. 67–82. ISSN: 0024-3795. DOI: [https://doi.org/10.1016/0024-3795\(87\)90103-0](https://doi.org/10.1016/0024-3795(87)90103-0).
- [5] Michael P. Connolly, Nicholas J. Higham, and Srikara Pranesh. *Randomized Low Rank Matrix Approximation: Rounding Error Analysis and a Mixed Precision Algorithm*. Tech. rep. 2022.10. The University of Manchester, 2022.
- [6] James W. Demmel et al. “Communication Avoiding Rank Revealing QR Factorization with Column Pivoting”. In: *SIAM Journal on Matrix Analysis and Applications* 36.1 (2015), pp. 55–89. DOI: [10.1137/13092157X](https://doi.org/10.1137/13092157X).
- [7] Monica Dessoale and Fabio Marcuzzi. “Deviation Maximization for Rank-Revealing QR Factorizations”. In: *Numer. Algorithms* 91.3 (Nov. 2022), pp. 1047–1079. ISSN: 1017-1398. DOI: [10.1007/s11075-022-01291-1](https://doi.org/10.1007/s11075-022-01291-1).
- [8] Zlatko Drmač and Zvonimir Bujanović. “On the Failure of Rank-Revealing QR Factorization Software – A Case Study”. In: *ACM Trans. Math. Softw.* 35.2 (July 2008). ISSN: 0098-3500. DOI: [10.1145/1377612.1377616](https://doi.org/10.1145/1377612.1377616).
- [9] Jed A. Duersch and Ming Gu. “Randomized QR with Column Pivoting”. In: *SIAM Journal on Scientific Computing* 39.4 (2017), pp. C263–C291. DOI: [10.1137/15M1044680](https://doi.org/10.1137/15M1044680).
- [10] Carl Eckart and Gale Young. “The approximation of one matrix by another of lower rank”. In: *Psychometrika* 1.3 (Sept. 1936), pp. 211–218. ISSN: 1860-0980. DOI: [10.1007/BF02288367](https://doi.org/10.1007/BF02288367).
- [11] Pieter Ghysels et al. “An Efficient Multicore Implementation of a Novel HSS-Structured Multifrontal Solver Using Randomized Sampling”. In: *SIAM Journal on Scientific Computing* 38.5 (2016), S358–S384. DOI: [10.1137/15M1010117](https://doi.org/10.1137/15M1010117).
- [12] Per Christian Hansen. “Regularization Tools version 4.0 for Matlab 7.3”. In: *Numerical Algorithms* 46.2 (Oct. 2007), pp. 189–194. ISSN: 1572-9265. DOI: [10.1007/s11075-007-9136-9](https://doi.org/10.1007/s11075-007-9136-9).
- [13] Nicholas Higham and Theo Mary. “A New Approach to Probabilistic Rounding Error Analysis”. In: *SIAM Journal on Scientific Computing* 41 (Jan. 2019), A2815–A2835. DOI: [10.1137/18M1226312](https://doi.org/10.1137/18M1226312).
- [14] Nicholas J. Higham. *Accuracy and Stability of Numerical Algorithms*. 2nd. USA: Society for Industrial and Applied Mathematics, 2002. ISBN: 0898715210.

- [15] Alston S. Householder. "Unitary Triangularization of a Nonsymmetric Matrix". In: *J. ACM* 5.4 (Oct. 1958), pp. 339–342. ISSN: 0004-5411. DOI: [10.1145/320941.320947](https://doi.org/10.1145/320941.320947).
- [16] W. Kahan. "Numerical Linear Algebra". In: *Canadian Mathematical Bulletin* 9.5 (1966), pp. 757–801. DOI: [10.4153/CMB-1966-083-2](https://doi.org/10.4153/CMB-1966-083-2).
- [17] R. B. Lehoucq. "The Computation of Elementary Unitary Matrices". In: *ACM Trans. Math. Softw.* 22.4 (Dec. 1996), pp. 393–400. ISSN: 0098-3500. DOI: [10.1145/235815.235817](https://doi.org/10.1145/235815.235817).
- [18] Edo Liberty et al. "Randomized algorithms for the low-rank approximation of matrices". In: *Proceedings of the National Academy of Sciences* 104.51 (2007), pp. 20167–20172.
- [19] Per-Gunnar Martinsson et al. "Householder QR Factorization With Randomization for Column Pivoting (HQRRP)". In: *SIAM Journal on Scientific Computing* 39.2 (2017), pp. C96–C115. DOI: [10.1137/16M1081270](https://doi.org/10.1137/16M1081270).
- [20] G. Pichon et al. "Sparse Supernodal Solver Using Block Low-Rank Compression". In: *2017 IEEE International Parallel and Distributed Processing Symposium Workshops (IPDPSW)*. May 2017, pp. 1138–1147. DOI: [10.1109/IPDPSW.2017.86](https://doi.org/10.1109/IPDPSW.2017.86).
- [21] R. Schreiber and C. Van Loan. "A storage-efficient WY representation for products of Householder transformations". In: *SIAM J. Sci. Stat. Comput.* 10 (1989), pp. 52–57.
- [22] Jianwei Xiao, Ming Gu, and Julien Langou. "Fast Parallel Randomized QR with Column Pivoting Algorithms for Reliable Low-Rank Matrix Approximations". In: *2017 IEEE 24th International Conference on High Performance Computing (HiPC)* (2017), pp. 233–242. URL: <https://api.semanticscholar.org/CorpusID:3444436>.



Institut de Recherche en Informatique de Toulouse
CNRS - INP - UT3 - UT1 - UT2J

ASR - Architecture, Systems and Networks

RMESS - Networks, Mobile, Embedded, Wireless, Sattellites

SEPIA - Operating systems, distributed systems, from Middleware to Architecture

SIERA - Service IntEgration and netwoRk Administration

T2RS - Real-Time in networks and systems

TRACES - Trace stands for research groups in architecture and compilation for embedded systems

CISO - HPC, Simulation, Optimization

APO - Parallel Algorithms and Optimisation

REVA - Real Expression Artificial Life

FSL - Reliability Systems and Software

ACADIE - Assistance for certification of distributed and embedded applications

ARGOS - Advancing Rigorous Software and System Engineering

ICS - Interactive Critical Systems

SM@RT - Smart Modeling for softw@re Research and Technology

GD - Data Management

IRIS - Information Retrieval and Information Synthesis

PYRAMIDE - Dynamic Query Optimization in large-scale distributed environments

SIG - Generalized information systems

IA - Artificial Intelligence

ADRIA - Argumentation, Decision, Reasoning, Uncertainty and Learning methods

LILaC - Logic, Interaction, Language and Computation

MELODI - Methods and Engineering of Language, Ontology and Discourse

ICI - Interaction, Collective Intelligence

ELIPSE - Human computer interaction

SMAC - Cooperative multi-agents systems

TALENT - Teaching And Learning Enhanced by Technologies

SI - Signals and Images

MINDS - coMputational Imaging and viSion

SAMoVA - Structuration, Analysis, Modeling of Video and Audio documents

SC - Signal and Communications

STORM - Structural Models and Tools in Computer Graphics

TCI - Images processing and understanding